Am J Transl Res 2020;12(11):7249-7261
www.ajtr.org /ISSN:1943-8141/AJTR0113709

Original Article

Platelet-activating factor induces the stemness of ovarian cancer cells via the PAF/PAFR signaling pathway

Tong Gao[1,2], Ran Zhao[3], Liangqing Yao[1,2], Congjian Xu[1,2], Qing Cong[1,2], Wei Jiang[1,2]

[1]Department of Gynecology, Obstetrics and Gynecology Hospital of Fudan University, Shanghai 200011, People's Republic of China; [2]Shanghai Key Laboratory of Female Reproductive Endocrine Related Diseases, Shanghai 200011, People's Republic of China; [3]Department of Respiratory, Shanghai Children's Hospital, Shanghai Jiaotong University, No. 355 Luding Road, Shanghai 200062, People's Republic of China

Received May 3, 2020; Accepted October 24, 2020; Epub November 15, 2020; Published November 30, 2020

Abstract: Background: Cancer stem cells (CSCs) play an important role in tumor recurrence, metastasis, and chemoresistance. CSCs can shift between non-CSC and CSC states in certain tumor microenvironments. The mechanisms of this shift are not well understood. We previously demonstrated that platelet-activating factor (PAF), a lipid mediator of inflammation in the tumor microenvironment, can promote ovarian cancer progression and induce chemoresistance via PAF/PAFR-mediated inflammatory signaling pathways. Here, we investigated the role of PAF/PAFR signaling in the stemness of ovarian cancer cell. Methods: The effects of PAF and PAFR antagonists on the stemness of SKOV3 and A2780 cells were evaluated using sphere-formation assays, FACS analysis and real-time PCR in vitro and a SKOV3 tumor-formation experiment in nude mice in vivo. The potential mechanism of the PAF effect on the stemness of ovarian cancer cells was evaluated by human cytokine antibody microarray analysis. Results: PAF can promote spheroid formation and inhibit the transition of quiescent ovarian cancer cells into the cell cycle. The percentage of cancer stem cells increased significantly, and the expression of stemness genes increased in PAF-treated group. These effects could be blocked by PAFR inhibitors. Ginkgolide B (GB) inhibited tumor growth and decreased the CSC percentage in vivo. Human cytokine antibody microarray analysis showed that some stemness-maintaining proteins increased in PAF-treated group. Conclusion: Our results suggest that PAF can regulate the stemness of ovarian cancer cells through the PAF/PAFR pathway, suggesting a new target for the treatment of ovarian cancer.

Keywords: PAF/PAFR signaling pathway, stemness, ovarian cancer

Introduction

Ovarian cancer is the most common gynecological malignancy and is the eighth most common cause of cancer in women. More than 75% of patients are diagnosed at late stages due to the incipient protracted nature of the disease and the lack of specific diagnostic symptoms or biomarkers. Despite aggressive surgical debulking and cytoreduction, 50-85% of patients experience recurrences with limited treatment options and poor survival [1-5].

Cancer stem cells (CSCs) are tumor cells that have the principal properties of self-renewal, clonal tumor initiation capacity and clonal long-term repopulation potential. In recent years, there has been increasing evidence that CSCs play an important role in tumor recurrence, metastasis, and chemoresistance [6]. Recent studies have indicated that chemotherapy can induce CSCs through a variety of mechanisms. Our previous study demonstrated that cisplatin induces the upregulation of PAFR in ovarian cancer cells. The blockade of PAFR can induce cell apoptosis and inhibit cell proliferation, promoting the efficacy of CDDP. Therefore, we believe that PAFR may regulate the stemness of ovarian cancer cells.

One of the hallmarks of cancer is the effect of inflammation on the tumor microenvironment [7]. In ovarian cancer, an inflammatory state is considered a risk factor and can be associated

Table 1. The primer sequences for RT-PCR

Klf4	Forward Primer	CCCACATGAAGCGACTTCCC
	Reverse Primer	CAGGTCCAGGAGATCGTTGAA
Nanog	Forward Primer	TTTGTGGGCCTGAAGAAAACT
	Reverse Primer	AGGGCTGTCCTGAATAAGCAG
Oct4	Forward Primer	CTGGGTTGATCCTCGGACCT
	Reverse Primer	CCATCGGAGTTGCTCTCCA
c-myc	Forward Primer	GGCTCCTGGCAAAAGGTCA
	Reverse Primer	CTGCGTAGTTGTGCTGATGT
CD24	Forward Primer	CTCCTACCCACGCAGATTTATTC
	Reverse Primer	AGAGTGAGACCACGAAGAGAC
CD34	Forward Primer	CTACAACACCTAGTACCCTTGGA
	Reverse Primer	GGAGAACACTGTGCTGATTACA
ALDH1	Forward Primer	GCACGCCAGACTTACCTGTC
	Reverse Primer	CCTCCTCAGTTGCAGGATTAAAG
Lgr5	Forward Primer	CTCCCAGGTCTGGTGTGTTG
	Reverse Primer	GAGGTCTAGGTAGGAGGTGAAG

with ovarian cancer development, drug resistance, and metastasis [8]. Platelet-activating factor (PAF), is one of the most potent inflammatory molecules [9]. PAFR is the main target of PAF. PAF/PAFR signaling is involved in oncogenic transformation, anti-apoptosis, metastasis and angiogenesis in several types of cancers [10]. We demonstrated that PAF/PAFR signaling is commonly activated in non-mucinous ovarian cancer cells and contributes to cancer progression and drug resistance [11]. Based on current reports, we postulated that PAF can regulate the stemness of ovarian cancer cells via the PAF/PAFR pathway [12].

In this study, we examine the effect of PAF on the stemness of SKOV3 and A2780 cells. The PAFR-specific antagonist Ginkgolide B (GB) and WEB2086 were found to inhibit cancer stemness in vitro and in vivo. Our results show that PAF can maintain cancer stemness via the PAF/PAFR pathway.

Materials and methods

Cell culture and chemical reagents

The ovarian cancer cell line SKOV3 and A2780 (purchased from the Cell Bank of the Chinese Academy of Science, Shanghai, China) were cultured at 37°C in a humidified 5% CO_2 atmosphere in RPMI-1640 medium with 10% fetal calf serum (Gibco, Invitrogen, Carlsbad, CA, USA) 100 IU/ml penicillin G and 100 mg/ml streptomycin sulfate (Sigma-Aldrich, St. Louis, MO, USA); the medium was changed every three days. Serum-free medium (DMEM/F12 medium with 2% B27 (Gibco, Invitrogen, Carlsbad, CA, USA), 20 ng/ml epidermal growth factor (R&D Systems, Oxon, U.K.), 20 ng/ml fibroblast growth factor (R&D Systems, Oxon, U.K.), 2 ng/ml heparin (R&D Systems, Oxon, U.K.), and 1% insulin (Gibco, Invitrogen, Carlsbad, CA, USA)) was used when measuring the stemness of ovarian cancer cells [13]. PAF, GB, and WEB2086 (PAFR antagonists) were purchased from Sigma-Aldrich.

Sphere-formation assay

The sphere-formation assay was performed as described previously [14]. Cells were plated in 24-well ultralow attachment plates (Corning Incorporated, Corning, NY, USA) at a density of 5000 cells per well and cultured in serum-free medium at 37°C in a humidified 5% CO_2 atmosphere. Cells were treated with 100 nmol/l PAF or 100 μmol/l WEB2086. After 14 days, the number of spheres (≥75 μm) was counted in all wells, and differences in the average number per well were evaluated.

RNA extraction and quantitative real-time PCR

Total RNA was isolated using TRIzol reagent (Invitrogen, USA) according to the manufacturer's instructions. Quantitative real-time PCR and real-time PCR analyses were performed with SYBR premix Ex Taq (TaKaRa, Osaka, Japan) on a 7900 Real-time PCR system (Applied Biosystems Inc., Foster, CA, USA) The conditions for qPCR were as follows: 95°C for 30 s; followed by 40 cycles at 95°C for 5 s and 60°C for 30 s; and a final cycle at 95°C for 5 s, 60°C for 1 min and 95°C with continuous mode. The primer sequences used for detection are shown in **Table 1**.

Flow cytometry

Surface marker expression: A2780 and SKOV3 cells were cultured with serum-free medium for 48 h and digested with trypsin enzyme, and then centrifuged at 350 g for 5 min at 4°C; the cell density was adjusted to 1×10^6 cells per assay for flow cytometric analysis. Cells were labeled with fluorochrome antibodies CD44-

FITC and CD133-APC (BD Bioscience). The experimental procedures were performed in accordance with a standard protocol on a CytoFLEX flow cytometer (Beckman Counter). The data are presented as the percentage of positive cells.

Cell cycle analysis: Treated cells were fixed in 70% ethanol and stored at 4°C overnight; the cells were labeled with propidium iodide (50 μg/ml) and RNase (100 μg/ml) for 30 min before flow cytometric analysis; the experiment was repeated for three times.

Western blot analysis: Cellular extracts were prepared in modified radioimmunoprecipitation assay (RIPA) buffer (50 mM Tris-HCl pH 7.4, 1% NP-40, 0.25% Na-deoxycholate, 150 mM NaCl, 1 mM EDTA, 1 mM PMSF, and protease inhibitor cocktail). The protein concentrations of the cellular extracts were measured using a Bio-Rad protein assay kit. Then, cellular extracts were subjected to SDS-PAGE. Proteins were transferred to PVDF membranes. After blocking for 1 h at room temperature in 5% BSA, the blots were probed with the primary antibody and incubated overnight at 4°C. Subsequently, the blots were washed three times and incubated for 1 h at room temperature with a 1:5000 dilution of secondary peroxidase-conjugated antibodies. The detection primary antibodies were: rabbit anti-human IGF-1R (1:100, CST 3024), rabbit anti-human SIGIRR (1:100, Abcam, ab177937), rabbit anti-human albumin (1:100, Abcam, ab151742), rabbit anti-human actin (1:100, CST, 3700). Following three washes, immunoreactive bands were detected using electrochemiluminescence (ECL).

Human cytokine antibody microarray analysis: SKOV3 cells were incubated in fresh serum-free medium overnight at 37°C in a humidified chamber with PAF (100 nM) treatment. Cells were harvested after 24 h of treatment by washing twice with phosphate-buffered saline (PBS) and then lysing with ice-cold cell lysis buffer (Cell Signaling Technology), supplemented with protease inhibitors. To simultaneously detect and semi-quantify 440 inflammatory markers in the cell lysates, G-Series Human Cytokine Antibody Array 440, from RayBiotech (Boechout, Belgium), was used. 40 μg of protein from cell lysates was incubated on the slide for 2 h and then incubated with a biotinylated antibody cocktail for 2 h, followed by incubation with the appropriate Cy3 dye-conjugated streptavidin label for 1 h. The signal intensity of each array was scanned using an InnoScan 300 Microarray Scanner (excitation frequency = 532 nm). The signal was analyzed with the microarray analysis software GSH-CAA-440. The different proteins were examined by Gene Ontology (GO) analysis and Kyoto Encyclopedia of Genes and Genomes (KEGG) enrichment pathway analysis.

Tumor formation in nude mice

Animals and treatment: All experimental procedures were conformed to the NIH Guide for the Care and Use of Laboratory Animals and were approved by the Animal Care and Use Committee of Fudan University. A total of 12 female BALB/c nude mice (4 to 6 weeks old) were obtained from the Laboratory Animal Center of the Shanghai Institutes for Biological Sciences of the Chinese Academy of Sciences, housed in a pathogen-free environment and used for ovarian cancer cell xenograft experiments. Xenografts were established by the subcutaneous injection of a total of 5×10^6 cells into the shoulder of each nude mouse. The animals were randomly divided into two groups. GB (Sigma) was dissolved in dimethyl sulfoxide (DMSO, Sigma) at a concentration of 10 mg/ml. The mice in the GB group were intraperitoneally injected with the PAFR antagonist GB for 14 days at a dose of 1 mg/mice.d (100 μl/d) for the duration of the animal experiment, while the mice in the control group were injected with DMSO (100 μl/d). Tumor sizes were measured 3 times per week. The tumors were measured using callipers, and tumor volumes were calculated using the following formula: tumor volume (mm^3) = (tumor length) × (tumor width)^2/2. The weights of the mice were recorded 3 times per week.

Preparation and analysis of tissues: The mice were euthanized by CO_2 inhalation followed by cervical dislocation. All the subcutaneous tumor tissues were removed, minced and incubated for 90 min in the presence of collagenase/hyaluronidase enzyme mix. After digestion, cell clumps were sieved through a 40-μm cell strainer (Falcon) to generate single-cell sus-

pensions, washed with PBS containing 2% FBS from plates, and centrifuged at 350 g at 4°C for 5 min, and the cell pellets were collected. The cell density was adjusted to 1×10^6 cells per assay for the flow cytometry assays. Cells were labeled with fluorochrome antibodies CD44-FITC and CD133-APC (BD Bioscience). The experimental procedures were performed in accordance with a standard protocol on a CytoFLEX flow cytometer (Beckman Counter). The data are presented as the percentage of positive cells.

Immunohistochemistry: Tumor tissue samples were fixed in 10% formalin and then paraffin embedded. Each tissue block was serially sectioned in 4-μm sections for further immunohistochemistry assays. The sections were dewaxed in xylene, rehydrated in graded alcohol, and rinsed in water. For antigen retrieval, the sections were immersed in 0.01 M of citrate buffer, pH 6.0, in a high-pressure cooker for 20 min, and the tissue sections were cooled at room temperature. A peroxidase block reagent was applied on the specimen according to the tissue size and it was incubated for 5-10 min at room temperature. After incubation with goat blocking serum for 15 min at room temperature, the processed slides were then incubated at 4°C overnight with the intended primary antibodies: dilution Ki-67 (1:100; Abcam ab245113) and CD34 (1:100; Abcam ab8158). After washing with PBS, the slides were incubated with horse radish peroxidase-labeled secondary antibody Detection Reagent (BioSun) and incubated at room temperature for 30 min. The resultant bound antibody complexes were stained with diaminobenzidine for 3-5 minutes or until appropriate for microscopic examination, followed by counterstaining with hematoxylin for 30 seconds, and then mounted. The staining images were procured with an Olympus microscope at 200 × magnification.

Statistical analysis

All statistical analyses were performed using GraphPad Prism 6.0. All experiments were performed at least three times. The data are expressed as the "mean ± SD". When appropriate, the data were subjected to unpaired two-tailed Student's t-tests. Differences were considered significant when $P < 0.05$.

Results

Effect of PAF on SKOV3 and A2780 spheroid formation and the inhibitory effects of WEB2086

Spheroid formation ability is considered a sign of self-renewal. CSCs have been reported to have a high ability to form spheroids in culture with serum-free media. To examine the sphere-forming ability of the reprogrammed cells, cells were plated in 24-well ultralow attachment plates and cultured for 14 days. As shown in **Figure 1A**, **1B** and Supplementary Figure 1A, 1B, PAF (100 nM) treatment enlarged the sphere numbers and sizes, and PAF promoted spheroid formation by SKOV3 and A2780. The promotion effect could be blocked by the PAFR-specific antagonist WEB2086 (100 μM). These data indicated that PAF promotes the spheroid formation ability of ovarian cancer cells at least in part via the PAF/PAFR pathway.

Effect of PAF on the cell cycle distribution of SKOV3 and A2780 cells and the expression of stemness genes and CSC markers

We examined the cell cycle distribution of SKOV3 and A2780 cells after treatment with PAF and WEB2086. As shown in **Figure 2** and Supplementary Figure 2, there was a significant increase in G0/G1-phase cells after PAF treatment compared with after DMSO or WEB2086 treatment. This cell cycle delay was accompanied by a decreased percentage of S-phase cells. Stem cells remain in the G0/G1 phase of the cell cycle for long periods of time; however, in our study, PAF inhibited the transition of quiescent ovarian cancer cells into the cell cycle [15]. The effect of PAF on stemness-related gene expression was examined. SKOV3 and A2780 cells were treated with PAF (100 nM), PAF (100 nM) + WEB2086 (100 μM) and WEB2086 (100 μM) for 24 h, and the expression of stemness genes were detected by RT-PCR. We observed an upregulation of the expression of several stemness genes (Oct4, nanog, klf4, c-myc, lgr5, CD24, CD34, and ALDH1) to varying degrees after PAF (100 nM) treatment for 24 h, as shown in **Figure 3** and Supplementary Figure 3. The promotion effect could be blocked by the PAFR-specific antagonist WEB2086 (100 μM). Next, the CSC markers of SKOV3 were examined after PAF and

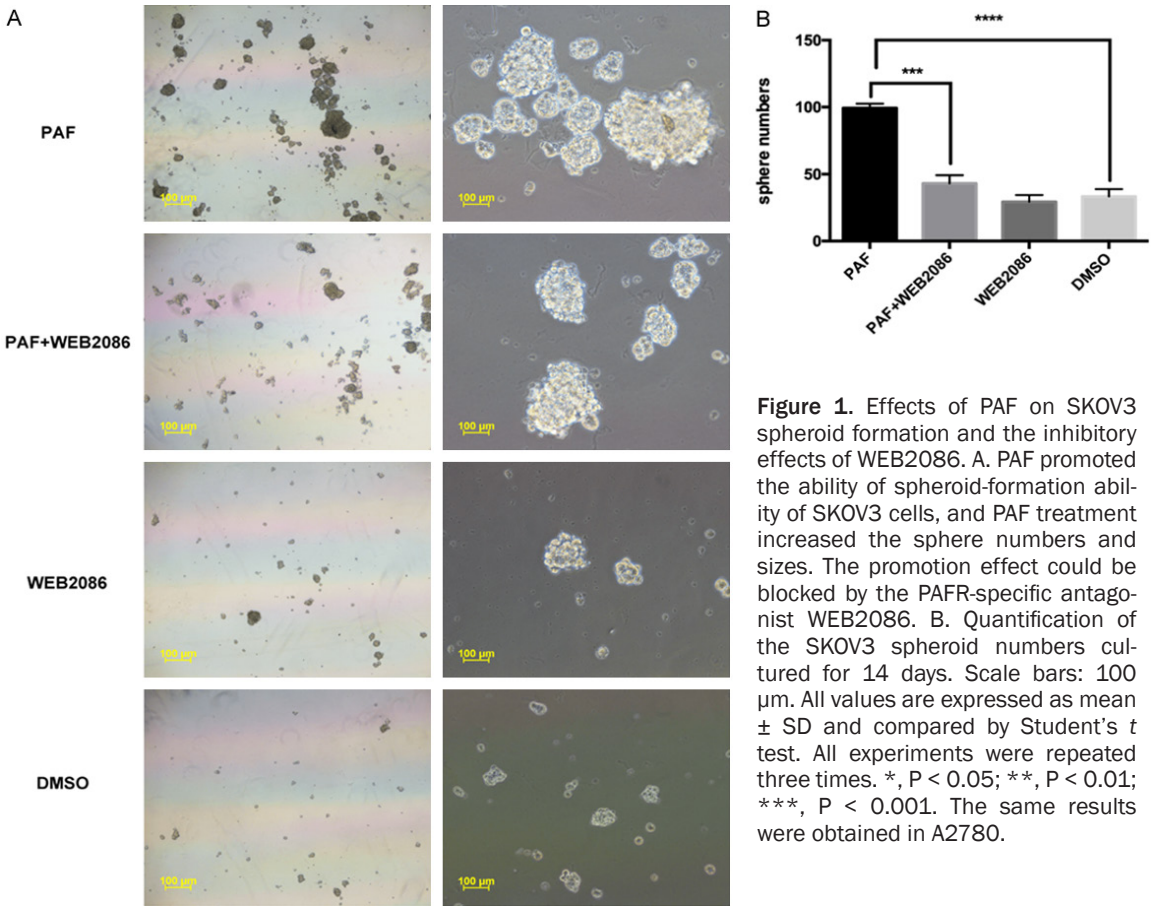

Figure 1. Effects of PAF on SKOV3 spheroid formation and the inhibitory effects of WEB2086. A. PAF promoted the ability of spheroid-formation ability of SKOV3 cells, and PAF treatment increased the sphere numbers and sizes. The promotion effect could be blocked by the PAFR-specific antagonist WEB2086. B. Quantification of the SKOV3 spheroid numbers cultured for 14 days. Scale bars: 100 μm. All values are expressed as mean ± SD and compared by Student's *t* test. All experiments were repeated three times. *, $P < 0.05$; **, $P < 0.01$; ***, $P < 0.001$. The same results were obtained in A2780.

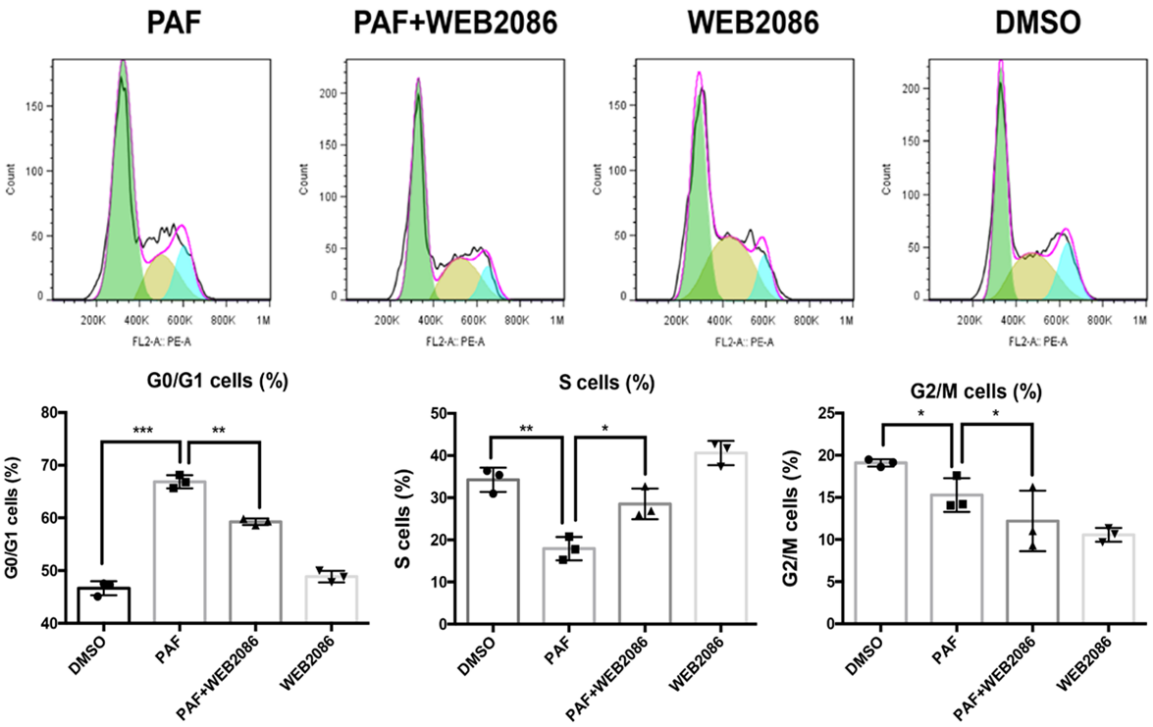

Figure 2. Effect of PAF on the SKOV3 cell cycle. PAF inhibited the transition of quiescent SKOV3 cells into the cell cycle. PAF treatment increased the percentage of G0/G1-phase cells. The cell cycle delay was accompanied by a

decreased percentage of S-phase cells. All values are expressed as mean ± SD and compared by Student's *t* test. All experiments were repeated three times. *, P < 0.05; **, P < 0.01; ***, P < 0.001. The same results were obtained in A2780.

WEB2086 treatment. We used CD44 and CD-133 as SKOV3 stem cell markers [16] and CD133 as the A2780 stem cell marker [17]. In SKOV3 cells, we observed a significant increase in the percentage of CD44+CD133+ cells after PAF (100 nM) treatment (**Figure 4A**, **4B**), and in A2780, we observed a significant increase in the percentage of CD133+ cells after PAF (100 nM) treatment (Supplementary Figure 4A, 4B). The promotion effect could also be blocked by the PAFR-specific antagonist WEB2086 (100 μM).

Human cytokine antibody microarray analysis

To further explore the potential underlying mechanism involved in the stemness of ovarian cancer cells after PAF treatment, we used a semi-quantitative protein array to examine protein expression in DMSO-treated and PAF-treated SKOV3 cells. The Raybiotech human GS440 array contains more than 440 antibodies raised against a wide variety of proteins representing a broad range of biological functions, including signal transduction, cell cycle regulation, gene transcription, and apoptosis. These arrays were used to examine protein expression in DMSO-treated and PAF-treated SKOV3 cells. By excluding the protein spots with inconsistent fold changes, we found that when we used a 1.5-fold cut-off, after treatment with PAF (100 nM), the protein levels of 19 proteins decreased, while that of 26 proteins increased, compared with DMSO (**Figure 5A**). A heatmap of protein expression was used for the visualization and validation of the results of the above protein selection. The heatmap of the expression levels of these 45 significant proteins clearly indicated that the protein expression pattern of the PAF-treated cells was different from that of the DMSO-treated cells. In the heatmap, the expression levels of the red-colored proteins were higher than those of the blue-colored proteins (**Figure 5B**). Western blotting was used to confirm the antibody microarray results of three proteins: albumin, IGF-1R and SIGIRR. Albumin and IGF-1R were significantly upregulated, whereas SIGIRR was significantly downregulated, in PAF-treated SKOV3 cells; these data were consistent with the antibody microarray results (**Figure 5C**). Whole membranes of Western blot was shown in Supplementary Figure 5. The differential proteins were analyzed by R; the top ten enriched GO terms are shown in **Figure 5D**. In addition, KEGG pathways were enriched in differential proteins, and the rich factor reflects the proportion of mutated genes in a given pathway (**Figure 5E**). The STRING database was used to determine the most relevant networks of the proteins altered by PAF treatment. According to the network analysis, the top canonical pathway was related to the ErbB and BMP receptor families (**Figure 5F**).

Effect of GB on the stemness of SKOV3 via the PAF/PAFR pathway in vivo

We finally investigated the in vivo activity of the PAFR antagonist GB in nude mice bearing SKOV3 cells that were grown subcutaneously as tumor xenografts. As shown in **Figure 6A**, **6C**, GB significantly inhibited the growth of SKOV3-derived subcutaneous tumors. The mouse weights recorded 3 times per week. Mice in the GB group had higher weights than did mice in the DMSO group (**Figure 6B**). As shown in **Figure 6D**, GB inhibited tumor growth and decreased the CSC percentage compared with the control group, and no obvious side effects were observed in the mice treated with GB. We investigated the effect of GB on the cell proliferation and blood vessel formation by immunohistochemistry. As shown in **Figure 6E**, we found slight decreases in Ki67 and CD34 in the GB-treated group, and GB can inhibit cell proliferation and angiogenesis in the ovarian cancer cells in vivo.

Discussion

Tumor heterogeneity is a major challenge to cancer therapy, and cancer stem-like cells are believed to explain intra-tumoral heterogeneity. CSCs are regarded as a subset of cancer cells that have self-renewal capacity and can initiate and maintain long-term tumor growth, generating cellular heterogeneity, which may be responsible for resistance to therapy, tumor recurrence and metastasis. CSCs are now thought to shift between non-CSC and CSC states, and this shift depends not only on

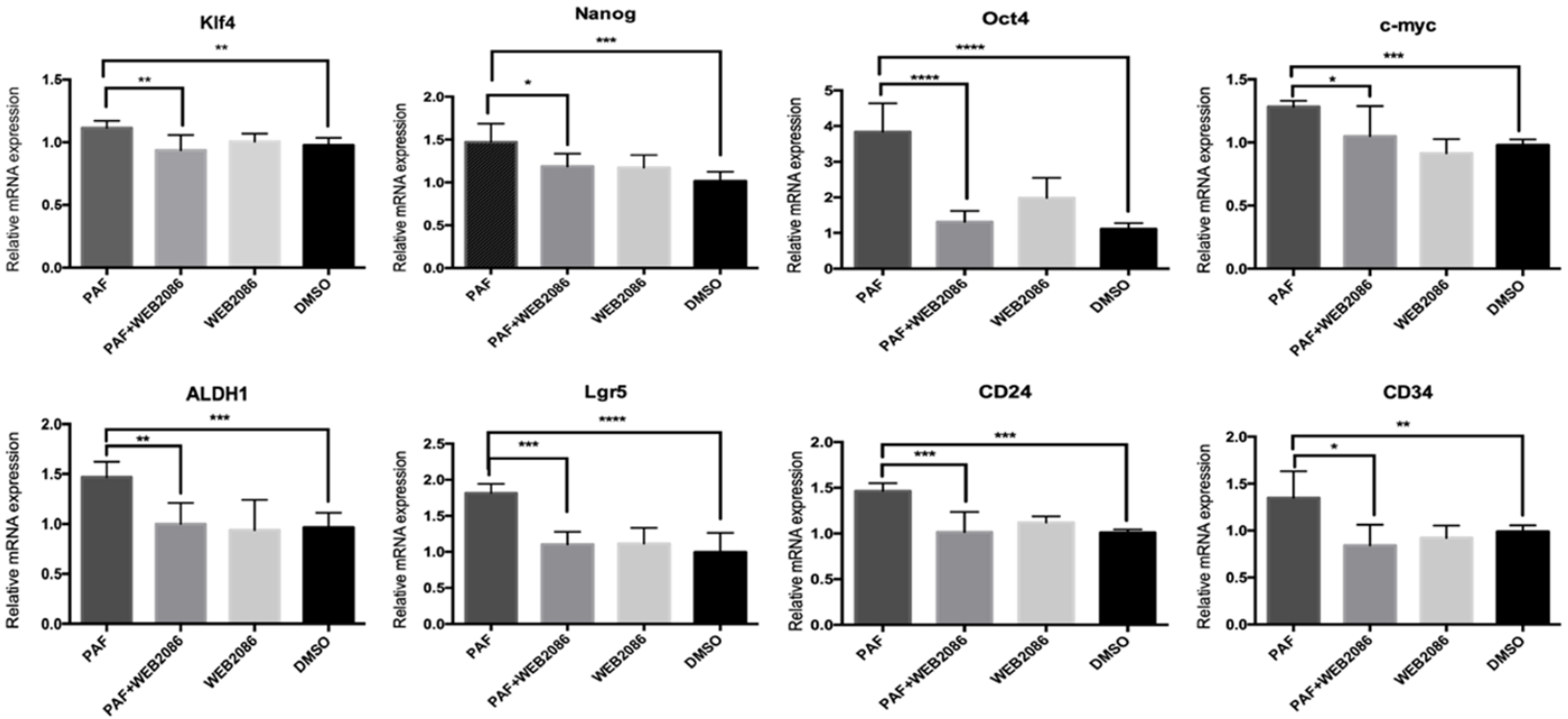

Figure 3. Effect of PAF on the stemness genes of SKOV3 cells. Significant upregulation of the expression of several stemness genes, such as Oct4, nanog, klf4, c-myc, lgr5, CD24, CD34, and ALDH1, was induced by PAF treatment. All values are expressed as mean ± SD and compared by Student's *t* test. All experiments were repeated three times. *, $P < 0.05$; **, $P < 0.01$; ***, $P < 0.001$. The same results were obtained in A2780.

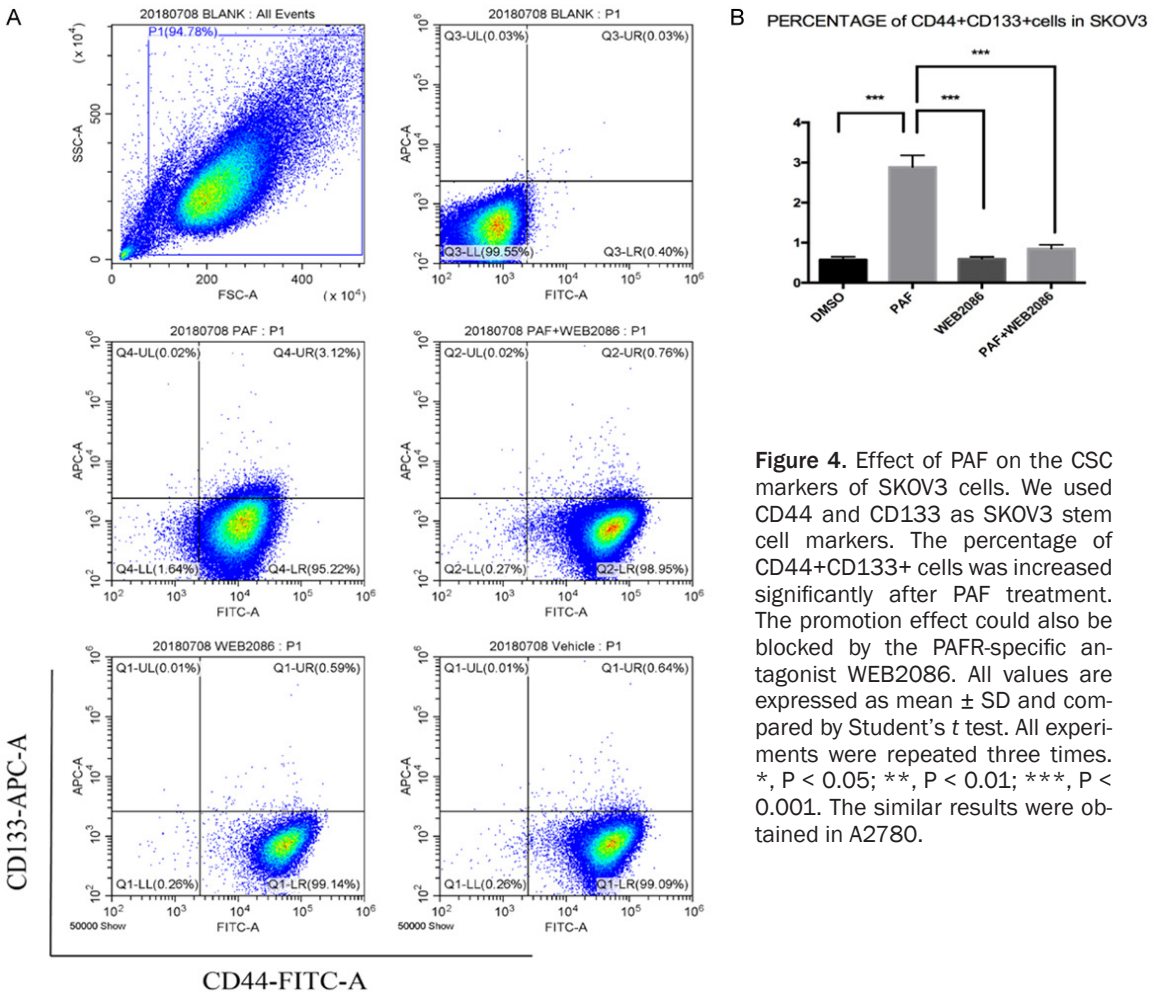

Figure 4. Effect of PAF on the CSC markers of SKOV3 cells. We used CD44 and CD133 as SKOV3 stem cell markers. The percentage of CD44+CD133+ cells was increased significantly after PAF treatment. The promotion effect could also be blocked by the PAFR-specific antagonist WEB2086. All values are expressed as mean ± SD and compared by Student's *t* test. All experiments were repeated three times. *, $P < 0.05$; **, $P < 0.01$; ***, $P < 0.001$. The similar results were obtained in A2780.

genetic and epigenetic alterations but also on signals provided by the tumor microenvironment and/or induced in response to therapy [18]. The stemness of cancer cells is controlled by many factors, and recent research has shown that the EMT is closely associated with CSCs. The stemness of cancer cells can be increased by TGF-β, HGF, EGF and FGF in the tumor microenvironment during EMT [19] and by EMT activators, such as those in the ZEB family [20]. CSCs are believed to reside in niches, which are specialized microenvironments that maintain the principle properties of CSCs and induce angiogenesis, and these CSCs recruit immune and other stromal cells that secrete additional factors to promote tumor cell invasion and metastasis [21].

Recent studies have indicated that chemotherapy can induce CSCs through a variety of mechanisms [22, 23]. For example, chemotherapy-induced hypoxia-inducible factors (HIFs) enrich CSCs through IL-6 and IL-8 signaling [24]. Additionally, chemotherapy can activate Wnt signals in hypoxic regions, while a chemotherapy-associated NF-kB-IL6-dependent inflammatory environment can endow non-stem cancer cells with stem-like features [25]. Moreover, chemotherapy was shown to induce additional Oncostatin M secretion, which may exacerbate the aggressive characteristics and treatment resistance of CSCs [26]; chemotherapy-induced senescence can alter the stem cell-related properties of malignant cells [27].

Our previous studies have shown that PAFR is highly expressed in serous, clear cell and endometrioid ovarian cancer cells; moreover, PAF can activate downstream signaling pathways via PAFR or transactivate EGFR and promote the proliferation and invasion of ovarian cancer cells [12, 28]. Additionally, PAF can modulate the cisplatin sensitivity of ovarian cancer cells [12, 29].

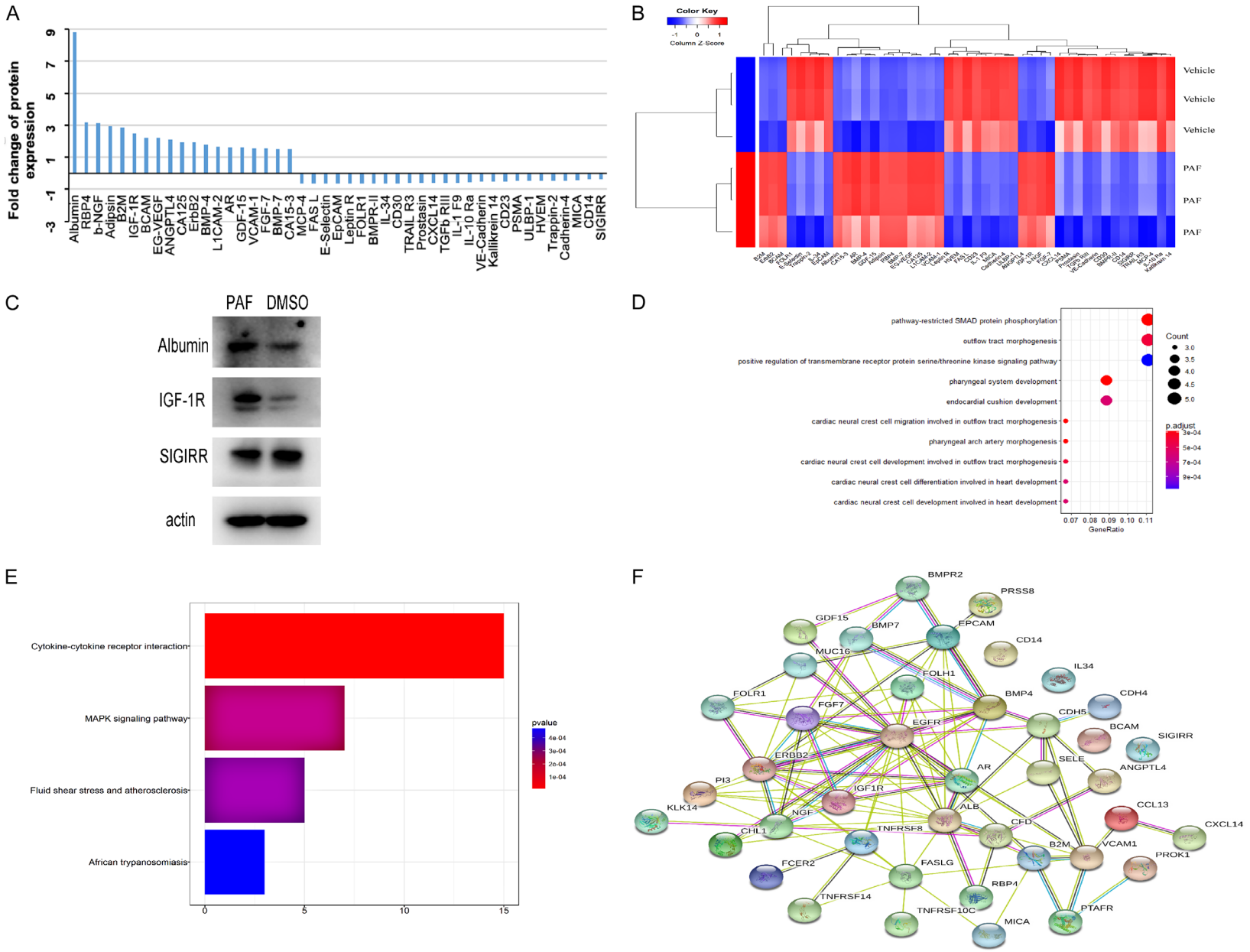
A
Fold change of protein expression
9
7
5
3
1
-1
-3
Albumin
RBP4
b-NGF
Adipsin
B2M
IGF-1R
BCAM
EG-VEGF
ANGPTL4
CA125
ErbB2
BMP-4
L1CAM-2
AR
GDF-15
VCAM-1
FGF-7
BMP-7
CA15-3
MCP-4
FAS L
E-Selectin
EpCAM
Leptin R
FOLR1
BMPR-II
IL-34
CD30
TRAIL R3
Prostasin
CXCL14
TGFb RIII
IL-1 F9
IL-10 Ra
VE-Cadherin
Kallikrein 14
CD23
PSMA
ULBP-1
HVEM
Trappin-2
Cadherin-4
MICA
CD14
SIGIRR
B
Color Key
-1
0
1
Column Z-Score
Vehicle
Vehicle
Vehicle
PAF
PAF
PAF
C
PAF
DMSO
Albumin
IGF-1R
SIGIRR
actin
D
pathway-restricted SMAD protein phosphorylation
outflow tract morphogenesis
positive regulation of transmembrane receptor protein serine/threonine kinase signaling pathway
pharyngeal system development
endocardial cushion development
cardiac neural crest cell migration involved in outflow tract morphogenesis
pharyngeal arch artery morphogenesis
cardiac neural crest cell development involved in outflow tract morphogenesis
cardiac neural crest cell differentiation involved in heart development
cardiac neural crest cell development involved in heart development
0.07
0.08
0.09
0.10
0.11
GeneRatio
Count
3.0
3.5
4.0
4.5
5.0
p.adjust
3e-04
5e-04
7e-04
9e-04
E
Cytokine-cytokine receptor interaction
MAPK signaling pathway
Fluid shear stress and atherosclerosis
African trypanosomiasis
0
5
10
15
pvalue
4e-04
3e-04
2e-04
1e-04
F
BMPR2
PRSS8
GDF15
BMP7
EPCAM
CD14
MUC16
IL34
FOLH1
FOLR1
BMP4
CDH4
FGF7
CDH5
EGFR
BCAM
SIGIRR
ERBB2
SELE
ANGPTL4
AR
PI3
IGF1R
KLK14
ALB
CCL13
NGF
CFD
CXCL14
CHL1
TNFRSF8
B2M
VCAM1
PROK1
FCER2
FASLG
RBP4
TNFRSF14
TNFRSF10C
PTAFR
MICA

Figure 5. Human cytokine antibody microarray analysis. A. Graphical presentation of the altered proteins in SKOV3 treated with PAF or DMSO. Among the 45 detected proteins, 19 were increased, and 26 were decreased. B. Two-dimensional hierarchical cluster analysis of differential proteins, which were significantly altered in response to PAF treatment. C. Western blotting analysis of albumin, IGF1R, and SIGIRR expression in SKOV3 cells treated with equal volumes of dimethyl sulfoxide (DMSO) or 100 nmol/l PAF for 24 h. Albumin, and IGF1R were upregulated, whereas SIGIRR was downregulated after PAF treatment. D. The top ten GO terms enriched in differential proteins analyzed by R. E. The KEGG pathways enriched in differential proteins. The rich factor reflects the proportion of mutated genes in a given pathway. F. Protein network of the identified proteins constructed with the STRING database.

Based on these studies, our results suggest a novel mechanism in terms of the inflammation microenvironment by which CSCs can be induced by the high concentration of PAF in the tumor microenvironment.

In this study, we explored whether PAF could induce the stemness of ovarian cancer through the PAF/PAFR signaling pathway and whether PAFR antagonists could be a useful adjuvant therapeutic approach with a possible inhibitory effect on CSCs. To this end, we used the PAF and PAFR-specific antagonists GB and WEB2086, respectively, and examined the in vitro and in vivo effects on sphere formation, CSC markers and tumor growth in mice.

Our in vitro results clearly indicated that PAF could promote spheroid formation and inhibit the transition of quiescent SKOV3 cells into the cell cycle. The promotion effect could be blocked by PAFR-specific antagonist WEB2086. PAF could promote the stemness of ovarian cancer, the percentage of CD44+CD133+ cells and several stemness genes, namely, Oct4, nanog, klf4, c-myc, lgr5, CD24, CD34, and ALDH1 were upregulated significantly by PAF. Combined with our previous results, our data indicate that high PAF concentrations in the tumor microenvironment can upregulate the stemness of SKOV3 in vitro and in vivo through the PAF/PAFR signaling pathway [26, 27, 41]. In addition, we found that many proteins that maintain stemness, such as such as RBP4 [30], IGF-1R [31], BMP4 [32], BMP7 [33], ErbB2 [34], ErbB3 [35], ANGPTL3 [36], VEGFR2 [37], uPAR [38], ADAM12 [39], RANK [40], and MMP10 [41], were upregulated to varying degrees. Our network analysis reviewed the top canonical pathway was related to the ErbB and BMP receptor families. BMP signaling participated in CSC-related tumor maintenance and progression by influencing the CSCs' functional properties, such as self-renewal, chemo-resistance, and tumor-initiating capacities in many cancers through BMP/Hedgehog signaling pathway and cross talk with Notch pathway and the Wnt pathway. ErbB family, especially EGFR, played an important role in the stemness of cancers through cross-talk with IGF-1R, activation of mitogen-activated protein kinases (MAPKs) and phosphorylated Akt in many cancers. GO analysis and Kyoto Encyclopedia of Genes and Genomes (KEGG) enrichment pathway analysis indicated that most proteins were enriched in the MAPK pathway and the PI3K/Akt signaling pathway.

Combined with our previous results, our data indicate that high PAF concentrations in the tumor microenvironment can promote the stemness of SKOV3 cells in vitro and in vivo through the PAF/PAFR signaling pathway. However, the mechanism involved in this process is unknown, and further studies are needed to investigate the exact mechanism to better understand the anti-tumor activity of GB.

Conclusion

The results of this study shed light on the cancer stemness-promoting effects of PAF on SKOV3 from a molecular perspective. Both in vitro and in vivo analyses suggest that the PAF/PAFR pathway plays an important role in the stemness of ovarian cancer. The specific PAFR inhibitors WEB2086 and GB may constitute a promising treatment strategy for non-mucinous ovarian cancer. A more thorough understanding of the role of PAFR in ovarian cancer is essential. Further studies are required to confirm the molecular mechanism underlying the effects of PAF and PAFR inhibitors on tumor stemness.

Acknowledgements

This work was supported by a grant from the National Natural Science Foundation of China (81672567) awarded to Wei Jiang.

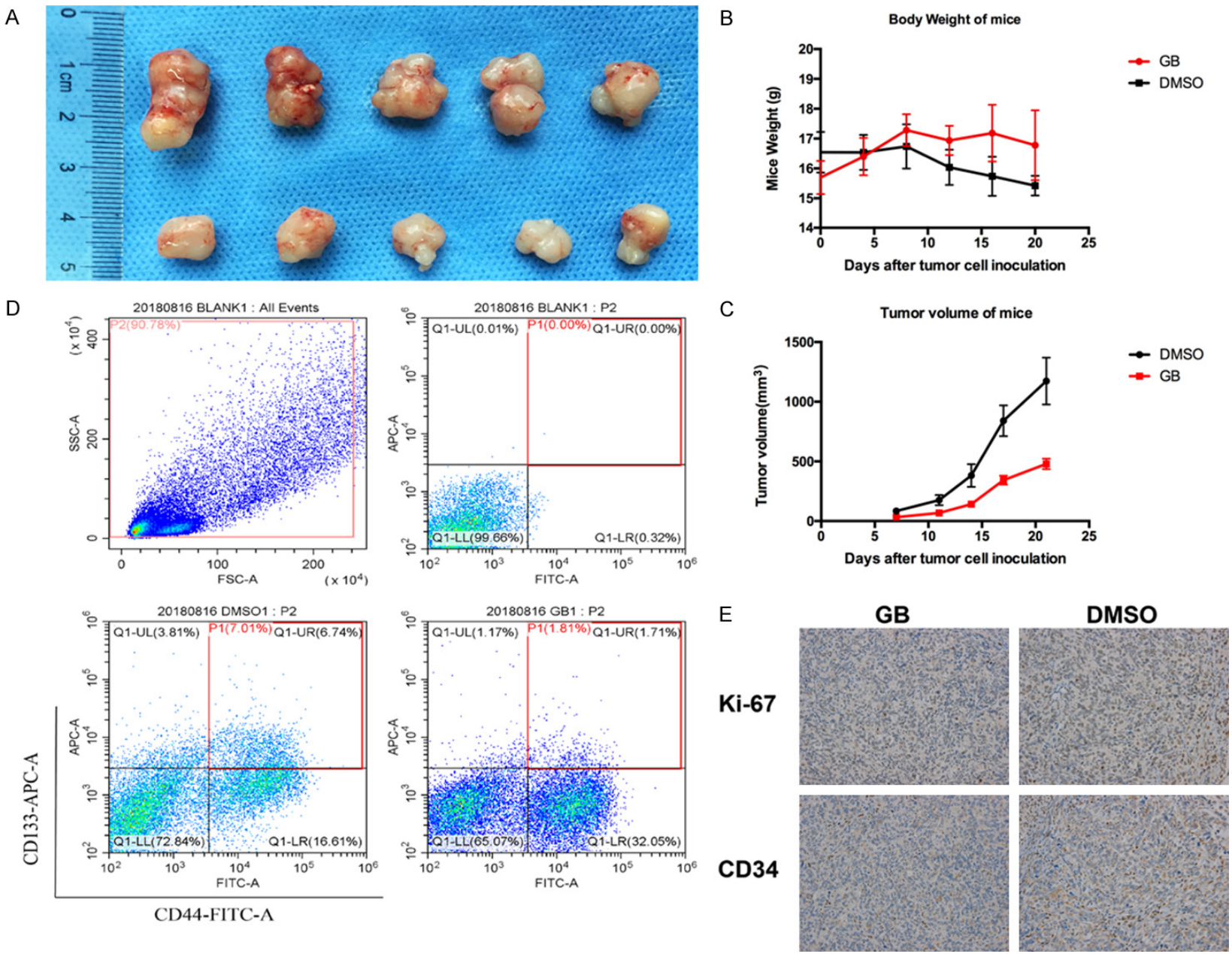
A
B
Body Weight of mice
GB
DMSO
Mice Weight (g)
Days after tumor cell inoculation
C
Tumor volume of mice
DMSO
GB
Tumor volume(mm3)
Days after tumor cell inoculation
D
20180816 BLANK1 : All Events
P2(90.78%)
SSC-A
FSC-A
20180816 BLANK1 : P2
Q1-UL(0.01%)
P1(0.00%)
Q1-UR(0.00%)
Q1-LL(99.66%)
Q1-LR(0.32%)
APC-A
FITC-A
20180816 DMSO1 : P2
Q1-UL(3.81%)
P1(7.01%)
Q1-UR(6.74%)
Q1-LL(72.84%)
Q1-LR(16.61%)
20180816 GB1 : P2
Q1-UL(1.17%)
P1(1.81%)
Q1-UR(1.71%)
Q1-LL(65.07%)
Q1-LR(32.05%)
CD133-APC-A
CD44-FITC-A
E
GB
DMSO
Ki-67
CD34

Figure 6. Effect of GB on the stemness of SKOV3 via the PAF/PAFR pathway in vivo. A. Representative photographs of tumors extracted from mice treated with or without GB (1 mg/mice, i.p., every day for two weeks). B. The ovarian tumor volume was determined in mice administered GB. C. The weight of each mouse was recorded 3 times per week. The mice in the GB group had higher weights than the mice in the DMSO group. D. GB decreased the CD44+CD133+ cells percentage, and no obvious side effects were observed in the mice treated with GB. E. Protein expression of Ki67 and CD34 in ovarian cancer tissues by immunohistochemistry, the expression of Ki67 and CD34 was decreased in the GB-treated group, which indicated GB inhibited cell proliferation and angiogenesis in the ovarian cancer cells in vivo. All values are expressed as mean ± SD and compared by Student's *t* test. All experiments were repeated three times. *, $P < 0.05$; **, $P < 0.01$.

Disclosure of conflict of interest

None.

Address correspondence to: Drs. Wei Jiang and Qing Cong, Department of Gynecology, Obstetrics and Gynecology Hospital, Fudan University, 419 Fangxie Road, Shanghai 200011, People's Republic of China. Tel: +86-021-63455050; Fax: +86-021-63455600; E-mail: jw52317@126.com (WJ); jennifercong@139.com (QC)

References

[1] Alharbi M, Zuniga F, Elfeky O, Guanzon D, Lai A, Rice GE, Perrin L, Hooper J and Salomon C. The potential role of miRNAs and exosomes in chemotherapy in ovarian cancer. Endocr Relat Cancer 2018; 25: R663-R685.

[2] Corrado G, Salutari V, Palluzzi E, Distefano MG, Scambia G and Ferrandina G. Optimizing treatment in recurrent epithelial ovarian cancer. Expert Rev Anticancer Ther 2017; 17: 1147-1158.

[3] Luvero D, Plotti F, Aloisia A, Montera R, Terranova C, De Cicco NC, Scaletta G, Lopez S, Miranda A, Capriglione S, Gatti A, Benedetti PP and Angioli R. Ovarian cancer relapse: from the latest scientific evidence to the best practice. Crit Rev Oncol Hematol 2019; 140: 28-38.

[4] Odunsi K. Immunotherapy in ovarian cancer. Ann Oncol 2017; 28: viii1-viii7.

[5] Pignata S, C Cecere S, Du Bois A, Harter P and Heitz F. Treatment of recurrent ovarian cancer. Ann Oncol 2017; 28: viii51-viii56.

[6] Tang C, Ang BT and Pervaiz S. Cancer stem cell: target for anti-cancer therapy. FASEB J 2007; 21: 3777-3785.

[7] Singh R, Mishra MK and Aggarwal H. Inflammation, immunity, and cancer. Mediators Inflamm 2017; 2017: 6027305.

[8] Kisielewski R, Tolwinska A, Mazurek A and Laudanski P. Inflammation and ovarian cancer--current views. Ginekol Pol 2013; 84: 293-297.

[9] Lynch JM, Lotner GZ, Betz SJ and Henson PM. The release of a platelet-activating factor by stimulated rabbit neutrophils. J Immunol 1979; 123: 1219-1226.

[10] Jancar S and Chammas R. PAF receptor and tumor growth. Curr Drug Targets 2014; 15: 982-987.

[11] Aponte M, Jiang W, Lakkis M, Li MJ, Edwards D, Albitar L, Vitonis A, Mok SC, Cramer DW and Ye B. Activation of platelet-activating factor receptor and pleiotropic effects on tyrosine phospho-EGFR/Src/FAK/paxillin in ovarian cancer. Cancer Res 2008; 68: 5839-5848.

[12] Yu Y, Zhang X, Hong S, Zhang M, Cai Q, Zhang M, Jiang W and Xu C. The expression of platelet-activating factor receptor modulates the cisplatin sensitivity of ovarian cancer cells: a novel target for combination therapy. Br J Cancer 2014; 111: 515-524.

[13] Valenti G, Quinn HM, Heynen G, Lan L, Holland JD, Vogel R, Wulf-Goldenberg A and Birchmeier W. Cancer stem cells regulate cancer-associated fibroblasts via activation of hedgehog signaling in mammary gland tumors. Cancer Res 2017; 77: 2134-2147.

[14] Chen X, Hu C, Zhang W, Shen Y, Wang J, Hu F and Yu P. Metformin inhibits the proliferation, metastasis, and cancer stem-like sphere formation in osteosarcoma MG63 cells in vitro. Tumour Biol 2015; 36: 9873-9883.

[15] Pacini N and Borziani F. Cancer stem cell theory and the warburg effect, two sides of the same coin? Int J Mol Sci 2014; 15: 8893-8930.

[16] Lee YJ, Wu CC, Li JW, Ou CC, Hsu SC, Tseng HH, Kao MC and Liu JY. A rational approach for cancer stem-like cell isolation and characterization using CD44 and prominin-1(CD133) as selection markers. Oncotarget 2016; 7: 78499-78515.

[17] Xiang T, Long H, He L, Han X, Lin K, Liang Z, Zhuo W, Xie R and Zhu B. Interleukin-17 produced by tumor microenvironment promotes self-renewal of CD133+ cancer stem-like cells in ovarian cancer. Oncogene 2015; 34: 165-176.

[18] Plaks V, Kong N and Werb Z. The cancer stem cell niche: how essential is the niche in regulating stemness of tumor cells? Cell Stem Cell 2015; 16: 225-238.

[19] Albini A, Bruno A, Gallo C, Pajardi G, Noonan DM and Dallaglio K. Cancer stem cells and the tumor microenvironment: interplay in tumor

heterogeneity. Connect Tissue Res 2015; 56: 414-425.
[20] Zhou P, Li B, Liu F, Zhang M, Wang Q, Liu Y, Yao Y and Li D. The epithelial to mesenchymal transition (EMT) and cancer stem cells: implication for treatment resistance in pancreatic cancer. Mol Cancer 2017; 16: 52.
[21] Lau EY, Ho NP and Lee TK. Cancer stem cells and their microenvironment: biology and therapeutic implications. Stem Cells Int 2017; 2017: 3714190.
[22] Wiechert A, Saygin C, Thiagarajan PS, Rao VS, Hale JS, Gupta N, Hitomi M, Nagaraj AB, DiFeo A, Lathia JD and Reizes O. Cisplatin induces stemness in ovarian cancer. Oncotarget 2016; 7: 30511-30522.
[23] Hu X, Ghisolfi L, Keates AC, Zhang J, Xiang S, Lee DK and Li CJ. Induction of cancer cell stemness by chemotherapy. Cell Cycle 2012; 11: 2691-2698.
[24] Chen X, Liao R, Li D and Sun J. Induced cancer stem cells generated by radiochemotherapy and their therapeutic implications. Oncotarget 2017; 8: 17301-17312.
[25] Zhang S, Yang X, Wang L and Zhang C. Interplay between inflammatory tumor microenvironment and cancer stem cells. Oncol Lett 2018; 16: 679-686.
[26] Chang JC. Cancer stem cells: role in tumor growth, recurrence, metastasis, and treatment resistance. Medicine (Baltimore) 2016; 95: S20-25.
[27] Milanovic M, Fan DNY, Belenki D, Däbritz JHM, Zhao Z, Yu Y, Dörr JR, Dimitrova L, Lenze D, Monteiro Barbosa IA, Mendoza-Parra MA, Kanashova T, Metzner M, Pardon K, Reimann M, Trumpp A, Dörken B, Zuber J, Gronemeyer H, Hummel M, Dittmar G, Lee S and Schmitt CA. Senescence-associated reprogramming promotes cancer stemness. Nature 2018; 553: 96-100.
[28] Yu Y, Zhang M, Zhang X, Cai Q, Hong S, Jiang W and Xu C. Synergistic effects of combined platelet-activating factor receptor and epidermal growth factor receptor targeting in ovarian cancer cells. J Hematol Oncol 2014; 7: 39.
[29] Jiang W, Cong Q, Wang Y, Ye B and Xu C. Ginkgo may sensitize ovarian cancer cells to cisplatin: antiproliferative and apoptosis-inducing effects of ginkgolide b on ovarian cancer cells. Integr Cancer Ther 2014; 13: NP10-17.
[30] Karunanithi S, Levi L, DeVecchio J, Karagkounis G, Reizes O, Lathia JD, Kalady MF and Noy N. RBP4-STRA6 pathway drives cancer stem cell maintenance and mediates high-fat diet-induced colon carcinogenesis. Stem Cell Rep 2017; 9: 438-450.
[31] Chang WW, Lin RJ, Yu J, Chang WY, Fu CH, Lai A, Yu JC and Yu AL. The expression and significance of insulin-like growth factor-1 receptor and its pathway on breast cancer stem/progenitors. Breast Cancer Res 2013; 15: R39.
[32] Zhang L, Sun H, Zhao F, Lu P, Ge C, Li H, Hou H, Yan M, Chen T, Jiang G, Xie H, Cui Y, Huang X, Fan J, Yao M and Li J. BMP4 administration induces differentiation of CD133+ hepatic cancer stem cells, blocking their contributions to hepatocellular carcinoma. Cancer Res 2012; 72: 4276-4285.
[33] Bosukonda A and Carlson WD. Harnessing the BMP signaling pathway to control the formation of cancer stem cells by effects on epithelial-to-mesenchymal transition. Biochem Soc Trans 2017; 45: 223-228.
[34] Rack B, Bock C, Andergassen U and Doisneau-Sixou S. Hormone receptor status, erbB2 expression and cancer stem cell characteristics of circulating tumor cells in breast cancer patients. Histol Histopathol 2012; 27: 855-864.
[35] Jarde T, Kass L, Staples M, Lescesen H, Carne P, Oliva K, McMurrick PJ and Abud HE. ERBB3 Positively correlates with intestinal stem cell markers but marks a distinct non proliferative cell population in colorectal cancer. PLoS One 2015; 10: e0138336.
[36] Fan X, Gay FP, Lim FW, Ang JM, Chu PP, Bari S and Hwang WY. Low-dose insulin-like growth factor binding proteins 1 and 2 and angiopoietin-like protein 3 coordinately stimulate ex vivo expansion of human umbilical cord blood hematopoietic stem cells as assayed in NOD/SCID gamma null mice. Stem Cell Res Ther 2014; 5: 71.
[37] Zhao D, Pan C, Sun J, Gilbert C, Drews-Elger K, Azzam DJ, Picon-Ruiz M, Kim M, Ullmer W, El-Ashry D, Creighton CJ and Slingerland JM. VEGF drives cancer-initiating stem cells through VEGFR-2/Stat3 signaling to upregulate Myc and Sox2. Oncogene 2015; 34: 3107-3119.
[38] Sobrevals L, Mato-Berciano A, Urtasun N, Mazo A and Fillat C. uPAR-controlled oncolytic adenoviruses eliminate cancer stem cells in human pancreatic tumors. Stem Cell Res 2014; 12: 1-10.
[39] Duhachek-Muggy S, Qi Y, Wise R, Alyahya L, Li H, Hodge J and Zolkiewska A. Metalloprotease-disintegrin ADAM12 actively promotes the stem cell-like phenotype in claudin-low breast cancer. Mol Cancer 2017; 16: 32.
[40] Sisay M, Mengistu G and Edessa D. The RANK/RANKL/OPG system in tumorigenesis and metastasis of cancer stem cell: potential targets for anticancer therapy. Onco Targets Ther 2017; 10: 3801-3810.
[41] Justilien V, Regala RP, Tseng IC, Walsh MP, Batra J, Radisky ES, Murray NR and Fields AP. Matrix metalloproteinase-10 is required for lung cancer stem cell maintenance, tumor initiation and metastatic potential. PLoS One 2012; 7: e35040.

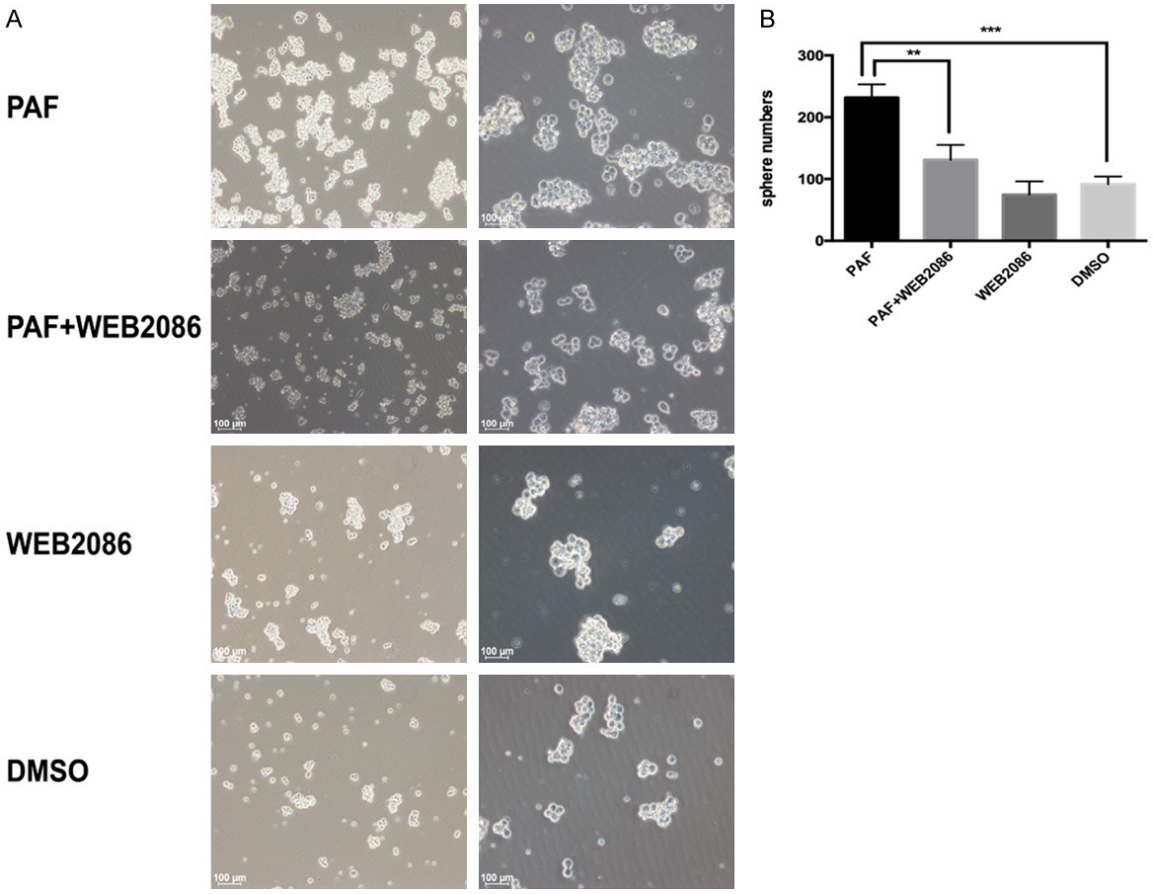

Supplementary Figure 1. Effects of PAF on A2780 spheroid formation and the inhibitory effects of WEB2086. A. PAF promoted the spheroid-formation ability of A2780, and PAF treatment increased the sphere numbers and sizes. The promotion effect could be blocked by the PAFR-specific antagonist WEB2086. B. Quantification of the A2780 spheroid numbers cultured for 14 days. Scale bars: 100 μm. All values are expressed as mean ± SD and compared by Student's *t* test. All experiments were repeated three times. *, P < 0.05; **, P < 0.01; ***, P < 0.001.

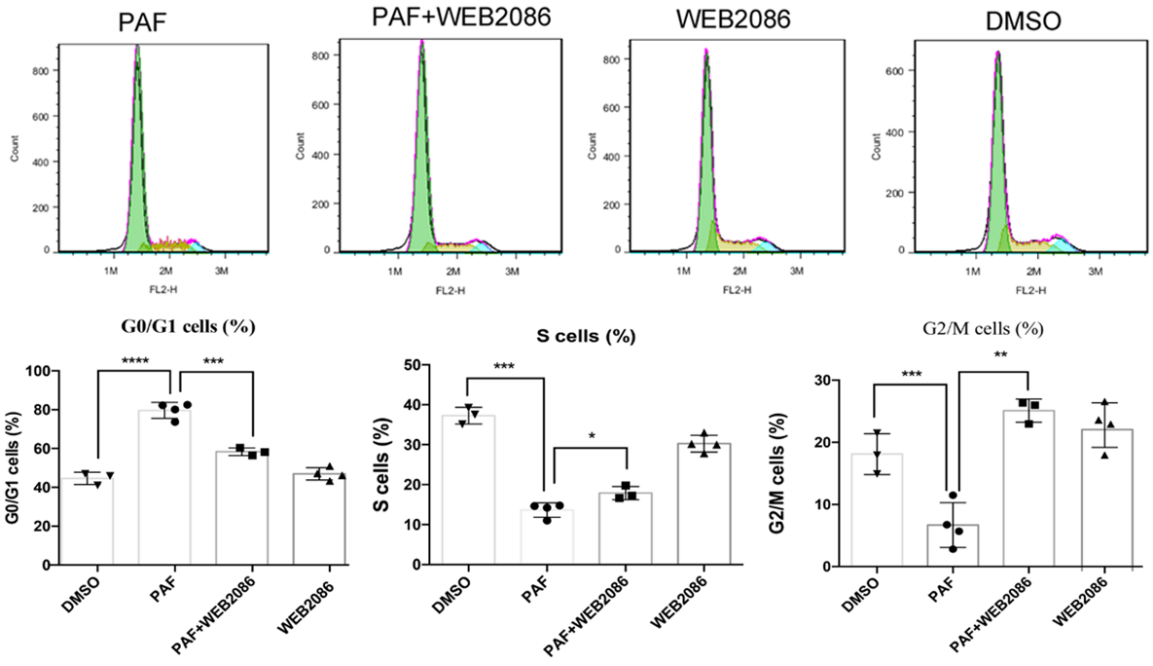

Supplementary Figure 2. Effect of PAF on the A2780 cell cycle. PAF inhibited the transition of quiescent A2780 cells into the cell cycle. PAF treatment increased the percentage of G0/G1-phase cells. The cell cycle delay was accompanied by a decreased percentage of S-phase cells. All values are expressed as mean ± SD and compared by Student's *t* test. All experiments were repeated three times. *, P < 0.05; **, P < 0.01; ***, P < 0.001.

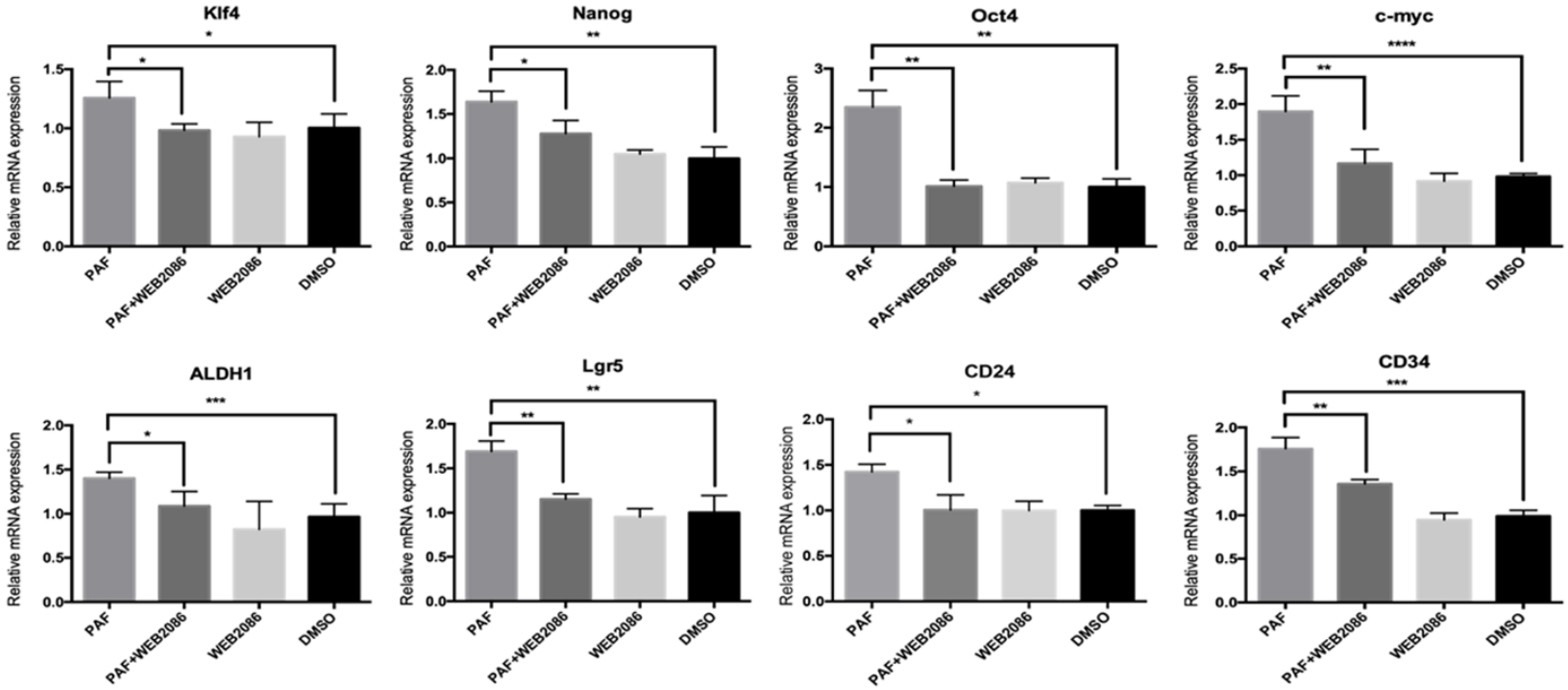

Supplementary Figure 3. Effect of PAF on the stemness genes of A2780 cells. Significant upregulation of the expression of several stemness genes, such as Oct4, nanog, klf4, c-myc, lgr5, CD24, CD34, and ALDH1, was induced by PAF treatment. All values are expressed as mean ± SD and compared by Student's *t* test. All experiments were repeated three times. *, P < 0.05; **, P < 0.01; ***, P < 0.001.

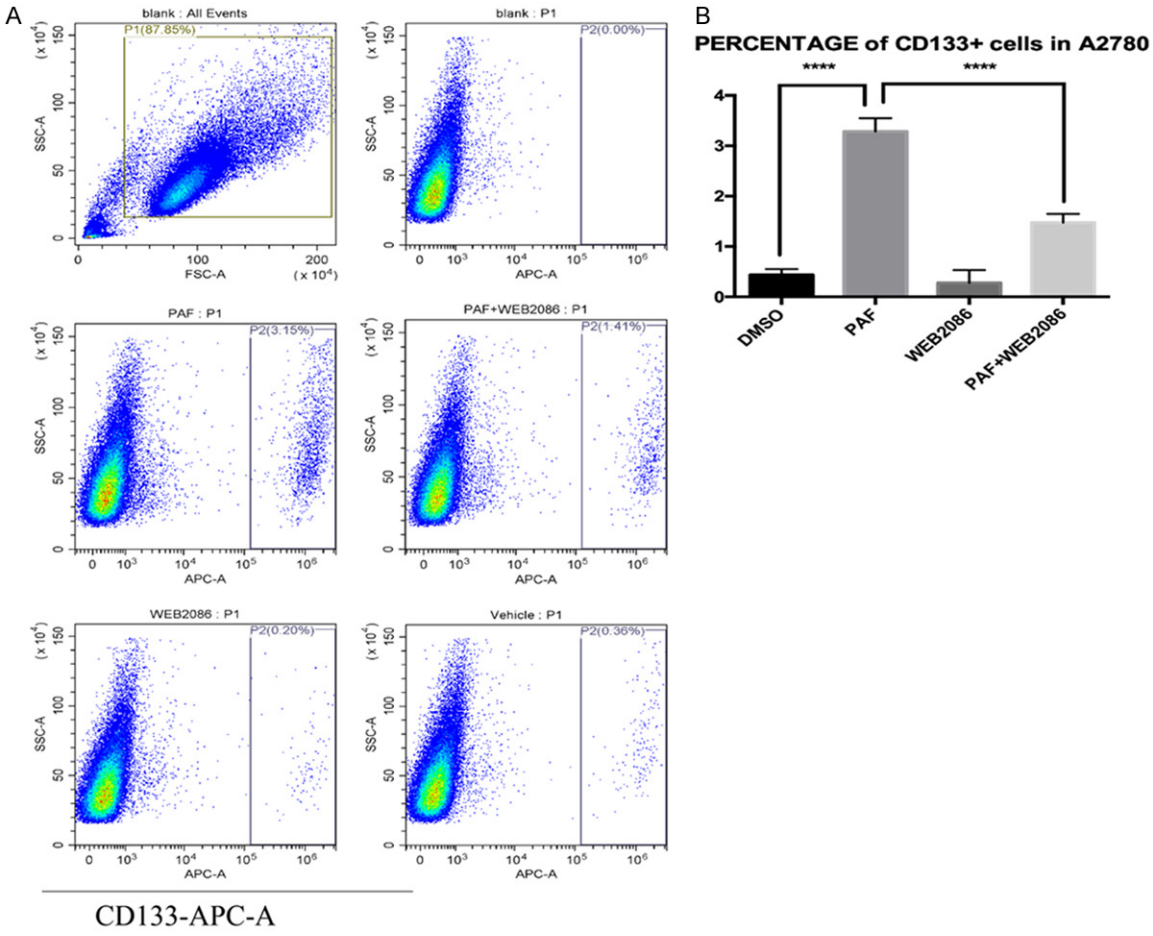

Supplementary Figure 4. Effect of PAF on the CSC markers of A2780 cells. We used CD133 as A2780 stem cell markers. The percentage of CD133+ cells was increased significantly after PAF treatment. The promotion effect could also be blocked by the PAFR-specific antagonist WEB2086. All values are expressed as mean ± SD and compared by Student's *t* test. All experiments were repeated three times. *, P < 0.05; **, P < 0.01; ***, P < 0.001.

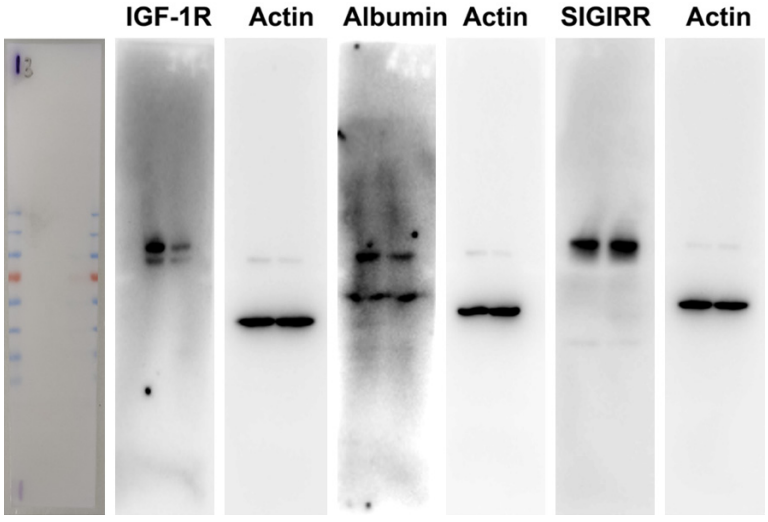

Supplementary Figure 5. Whole membranes of Western blot. Western blotting analysis of albumin, IGF1R, and SIGIRR expression in SKOV3 cells treated with equal volumes of dimethyl sulfoxide (DMSO) or 100 nmol/l PAF for 24 h. Albumin, and IGF1R were upregulated, whereas SIGIRR was downregulated after PAF treatment.